La théorie Bending-Gradient dans le code d'élément finis

Rawad Baroud, Karam Sab, Arthur Lebée

Modélisation élément finis des plaques multicouches en utilisant la théorie Bending-Gradient

Finite-Element Modeling of laminated plates using the Bending-Gradient theory

Rawad Baroud[1], Karam Sab[1] et Arthur Lebée[1]

1 : IFSTTAR, CNRS, Laboratoire Navier
ENPC, Université Paris-Est
77455 Marne-la-vallée, France
e-mail : rawad.baroud@enpc.fr, karam.sab@enpc.fr et arthur.lebee@enpc.fr

Résumé

Dans cet article, une modélisation par éléments finis d'une théorie de plaque récente pour les plaques épaisses chargées hors-plan, appelée la théorie du Bending-Gradient, est proposée. Cette théorie, qui a sept degrés de liberté (un déplacement transversal et six rotations généralisées), est une simplification de la théorie Generalized-Reissner qui s'étend à des plaques arbitraires multicouches que la théorie Reissner a initialement initiée pour des plaques homogènes. Un programme d'éléments finis appelé BGFEAP a été développé pour la mise en œuvre d'un nouvel élément à huit nœuds dédié à la théorie Bending-Gradient. Le modèle d'éléments finis proposé est capable de calculer la distribution des contraintes de cisaillement transverses dans l'épaisseur de la plaque. Plusieurs comparaisons sont effectuées entre les nouveaux modèles d'éléments finis Bending-Gradient, *LS1* et Abaqus éléments finis de plaques afin d'évaluer la performance du nouveau modèle qui se révèle très efficace pour les structures complexes.

Abstract

In this paper, a finite-element modeling of a recent plate theory for out-of-plane loaded thick plates, named the Bending-Gradient theory, is proposed. This theory, which has seven degrees of freedom (one transverse displacement and six generalized rotations), is a simplification of the Generalized-Reissner theory which extends to arbitrary multilayered plates the Reissner theory initially introduced for homogeneous plates. A finite-element program called BGFEAP has been developed for the implementation of a new eight-node element dedicated to Bending-Gradient theory. The proposed finite element model is capable of computing transverse shear stress distribution in the plate thickness. Several comparisons are made between the new Bending-Gradient finite-element, *LS1* layerwise finite-element model and Abaqus plate finite-element in order to assess the performance of the new model which shows itself very effective for complex structures.

Mots Clés : Théorie des plaques épaisses, Modèles d'ordre supérieur, Plaques laminées, Éléments Finis
Keywords : Thick Plate Theory, Higher-order Models, Laminated Plates, Finite-Element

1. Introduction

Laminated plates are being increasingly used in engineering applications such as civil engineering, aerospace ... However, as the constituents of these plates are generally very anisotropic materials, an efficient design of these structures requires dedicated numerical tools. In the light of a solid interest from industry for reliable models, numerous recommendations have been made, the main objective being to simplify a computationally heavy 3D model into a 2D plate model without losing local 3D fields' accuracy.

Two main approaches can be found in the literature to handle the effects of transverse shear stresses : asymptotic approaches and axiomatic approaches. The first class of approaches is mainly based on asymptotic expansions in the small parameter h/L. Such asymptotic approaches lead to models which are not simple to implement.

The second main class of approaches is based on assuming *ad hoc* displacement or stress 3D fields and it seems easier to implement in finite element codes. These models can be Equivalent Single Layer (ESL) or Layerwise. ESL models treat the whole laminate as an equivalent homogeneous plate. However, these models are restricted to some specific configurations (symmetry of the plate and

material constitutive equation) and involve higher-order partial derivative equations than the simple Reissner-Mindlin plate model. The difficulties encountered with transverse stress fields instigated the consideration of Layerwise models. In layerwise models, all plate degrees of freedom are introduced in each layer of the laminate and continuity conditions are enforced between layers. Layerwise models lead to correct estimates of local 3D fields. However, their main drawback is that they involve a number of degrees of freedom proportional to the number of layers than ESL models.
On the other hand, the extension of the original approach from Reissner [1] based on the principle of minimum complementary energy led to an Equivalent Single Layer plate theory called the Generalized-Reissner theory [2, 3]. This theory takes accurately into account shear effects and does not require any specific constitutive material symmetry. When suitably simplified, this theory becomes the Bending-Gradient theory already introduced in [4, 5, 6, 7, 8]. Here, shear forces are replaced by the gradient of the bending moment $\underset{\approx}{\boldsymbol{R}} = \underset{\sim}{\boldsymbol{M}} \otimes \underline{\boldsymbol{\nabla}}$. Hence, the Bending-Gradient theory belongs to the family of higher-order gradient models. The kinematic degrees of freedom (d.o.f.) are the deflection, and the generalized rotation which may have between two and six d.o.f.. Indeed, it was also established that, when the plate is homogeneous, then the original theory from Reissner [1] with three d.o.f. (one deflection, two rotations) is fully recovered.
Since the Bending-Gradient model is not yet implemented in finite element program and its usage is limited to analytical solutions [5, 9] used to calculate 1D models with some restrictions ; for this, the purpose of this paper is to present the finite element implementation of the Bending-Gradient model and to show its accuracy when compared to Bending-Gradient analytical model, ABAQUS composite layup plate finite element model, and *LS1* finite element layerwise model [10, 11, 12, 13, 14, 15, 16, 17, 18, 19, 20]

2. Notations

First, second, third, fourth and sixth order tensors are respectively noted : $\underline{\boldsymbol{X}}$, $\underline{\underline{\boldsymbol{X}}}$, $\underline{\underline{\underline{\boldsymbol{X}}}}$, $\underline{\underline{\underline{\underline{\boldsymbol{X}}}}}$ and $\underline{\underline{\underline{\underline{\underline{\underline{\boldsymbol{X}}}}}}}$. When dealing with plates, both 2D and 3D tensors are utilized. Thus, $\underline{\boldsymbol{X}}$ will denote a 3D vector or a 2D vector depending on its nature. The same convention is used for higher-order tensors. When using tensor components, the indices typeface specify the dimension : (X_{ij}) denotes the 3D tensor $\underline{\underline{\boldsymbol{X}}}$ with Latin indices $i, j, k.. = 1, 2, 3$ while $(X_{\alpha\beta})$ denotes the 2D tensor $\underline{\underline{\boldsymbol{X}}}$ with Greek indices $\alpha, \beta, \gamma.. = 1, 2$. The transpose operation ${}^{T}\bullet$ is applied to any order tensors as follows : $({}^{T}X)_{\alpha\beta\ldots\psi\omega} = X_{\omega\psi\ldots\beta\alpha}$. Five symbols are defined : $(\cdot)$, $(:)$, $(\vdots)$, $(\vdots)$ and $(\vdots\vdots)$ for contraction on, respectively, one, two, three, four and six indices. By convention, the closest indices are successively summed together in contraction products.
The identity for 2D vectors is $\underline{\boldsymbol{\delta}} = (\delta_{\alpha\beta})$ where $\delta_{\alpha\beta}$ is Kronecker symbol ($\delta_{\alpha\beta} = 1$ if $\alpha = \beta$, $\delta_{\alpha\beta} = 0$ otherwise). The identity for 2D symmetric fourth order tensors is $\underline{\underline{\underline{\underline{\boldsymbol{i}}}}}$ where $i_{\alpha\beta\gamma\delta} = \frac{1}{2}\left(\delta_{\alpha\gamma}\delta_{\beta\delta} + \delta_{\alpha\delta}\delta_{\beta\gamma}\right)$.
The gradient of a scalar field X writes $X\underline{\boldsymbol{\nabla}} = (X_{,\beta})$ and the gradient of vectors or higher order tensor fields writes $\underline{\boldsymbol{X}} \otimes \underline{\boldsymbol{\nabla}} = (X_{\alpha\beta,\gamma})$, where $\otimes$ is the dyadic product. The divergence of a vector field, a second-order tensor field, a third-order tensor field is noted $\underline{\boldsymbol{X}} \cdot \underline{\boldsymbol{\nabla}} = (X_{\alpha,\alpha})$, $\underline{\underline{\boldsymbol{X}}} \cdot \underline{\boldsymbol{\nabla}} = (X_{\alpha\beta,\beta})$ and $\underline{\underline{\underline{\boldsymbol{X}}}} \cdot \underline{\boldsymbol{\nabla}} = (X_{\alpha\beta\gamma,\gamma})$, respectively.

3. The 3D Problem

The plate occupies the volume $\Omega = \omega \times \mathcal{T}$ where ω denotes the mid-plane surface of the plate and $\mathcal{T} = \left]-\frac{t}{2}, \frac{t}{2}\right[$ is the transverse coordinate range. The boundary, $\partial\Omega$, is decomposed into three parts (Refer to Figure 1) :

$$\begin{gathered} \partial\Omega = \partial\Omega_{\text{lat}} \cup \partial\Omega_3^+ \cup \partial\Omega_3^-, \\ \text{with} \quad \partial\Omega_{\text{lat}} = \partial\omega \times \mathcal{T} \quad \text{and} \quad \partial\Omega_3^{\pm} = \omega \times \left\{\pm\frac{t}{2}\right\}. \end{gathered} \tag{Eq. 1}$$

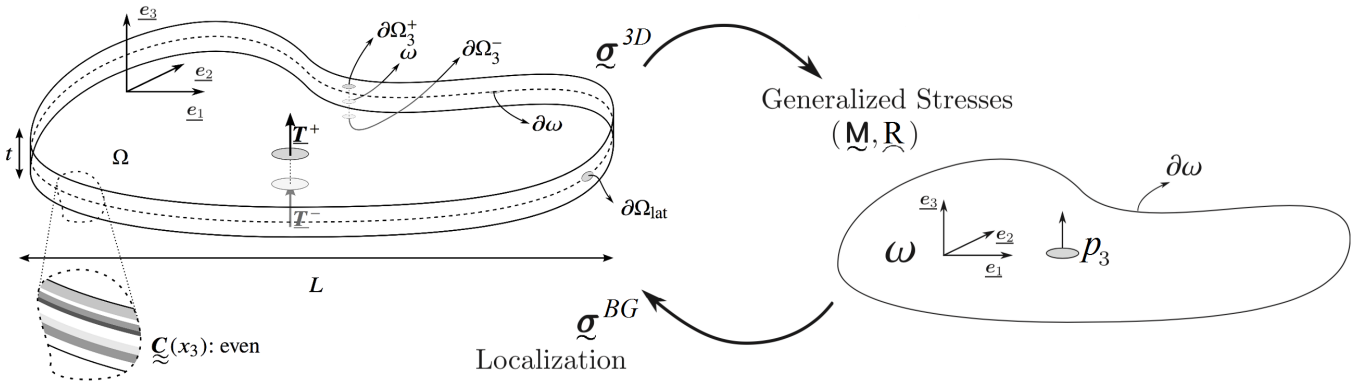

Fig. 1. Plate Configuration.

It is assumed that the local stiffness tensor $\underline{\underline{\underline{\underline{C}}}} = \left(C_{ijkl}\right)$ at every point $\underline{x} = (x_1, x_2, x_3)$ of Ω is invariant with respect to translations in the (x_1, x_2) plane and is an even function of x_3 : $\underline{\underline{\underline{\underline{C}}}}(x_3) = \underline{\underline{\underline{\underline{C}}}}(-x_3)$. The plate is clamped on its lateral boundary $\partial\Omega_{\text{lat}}$ (other conditions can be also considered) and is loaded with the out-of-plane distributed surface force $\frac{1}{2}p_3\,(x_1, x_2)$ along x_3 direction on both faces $\partial\Omega_3^{\pm}$.
The compliance tensor $\underline{\underline{\underline{\underline{S}}}} = \underline{\underline{\underline{\underline{C}}}}^{-1}$ follows the classical symmetries of linear elasticity and it is positive definite. In addition, monoclinic symmetry is assumed :$S_{3\alpha\beta\gamma} = S_{\alpha 333} = 0$.
Thus, the constitutive equation writes as :

$$\varepsilon_{\alpha\beta} = S_{\alpha\beta\gamma\delta}\sigma_{\delta\gamma} + S_{\alpha\beta 33}\sigma_{33}, \quad \varepsilon_{\alpha 3} = 2S_{\alpha 3\beta 3}\sigma_{3\beta}, \quad \varepsilon_{33} = S_{33\alpha\beta}\sigma_{\beta\alpha} + S_{3333}\sigma_{33}, \qquad \text{(Eq. 2)}$$

where $\underline{\underline{\sigma}} = \left(\sigma_{ij}\right)$ is the stress tensor and $\underline{\underline{\varepsilon}} = \left(\varepsilon_{ij}\right)$ is the strain tensor. The following notations are needed for the partial compliance tensors : $\underline{\underline{\underline{\underline{S}}}}^{\sigma} = \left(S_{\alpha\beta\gamma\delta}\right)$, $\underline{\underline{\underline{\underline{C}}}}^{\sigma} = \left(\underline{\underline{\underline{\underline{S}}}}^{\sigma}\right)^{-1}$, $\underline{\underline{S}}^{\gamma} = \left(4S_{\alpha 3\beta 3}\right)$, $\underline{\underline{S}}^{\nu} = \left(S_{\alpha\beta 33}\right)$, where $\underline{\underline{\underline{\underline{S}}}}^{\sigma}$ corresponds to plane stress compliance, $\underline{\underline{\underline{\underline{C}}}}^{\sigma}$ to plane stress stiffness, $\underline{\underline{S}}^{\gamma}$ to transverse shear compliance and $\underline{\underline{S}}^{\nu}$ is the out-of-plane Poisson coupling.
From the symmetries of the problem it can be established that the 3D solution components $\sigma^{3D}_{\alpha\beta}$, σ^{3D}_{33}, $\varepsilon^{3D}_{\alpha\beta}$, ε^{3D}_{33} and u^{3D}_{α} are odd in x_3 while $\sigma^{3D}_{\alpha 3}$, $\varepsilon^{3D}_{\alpha 3}$ and u^{3D}_{3} are even in x_3 ($\underline{u}^{3D}$ is the 3D displacement).

4. The Bending-Gradient theory

The Generalized-Reissner theory of [2, 3] is the extension to laminates of Reissner theory for homogeneous and isotropic plates [1]. However, it involves fifteen kinematic degrees of freedom (d.o.f.), eight of them being related only to out-of-plane Poisson's distortion, not really interesting for engineering applications. Thus, the main idea of the Bending-Gradient plate theory, initially introduced in [4, 5], is to simplify the Generalized-Reissner theory by setting these eight d.o.f. to zero and to neglect the contribution of the normal stress σ_{33} in the plate model constitutive equation.

4.1. The Bending-Gradient equations

The Bending-Gradient theory has seven d.o.f. : $\left(U_3, \underline{\underline{\underline{\mathbf{\Phi}}}}\right)$ where the scalar U_3 is the out-of-plane displacement and $\underline{\underline{\underline{\mathbf{\Phi}}}} = \left(\Phi_{\alpha\beta\gamma}\right)$ with $\Phi_{\alpha\beta\gamma} = \Phi_{\beta\alpha\gamma}$ is the generalized third-order rotation tensor.
The Bending-Gradient generalized strains, dual of the generalized stresses $\left(\underline{\underline{M}}, \underline{\underline{R}}\right)$, are $\left(\underline{\underline{\chi}}, \underline{\underline{\Gamma}}\right)$, with $M_{\alpha\beta} = M_{\beta\alpha}$ and $R_{\alpha\beta\gamma} = R_{\beta\alpha\gamma}$, where $\underline{\underline{\chi}}$ is the curvature and $\underline{\underline{\Gamma}}$ is the generalized shear strain. These generalized strains derive from the generalized displacements $\left(U_3, \underline{\underline{\underline{\mathbf{\Phi}}}}\right)$ using the following

compatibility conditions on ω :

$$\underset{\sim}{\boldsymbol{\chi}} = \underset{\frown}{\boldsymbol{\Phi}} \cdot \underline{\boldsymbol{\nabla}}, \quad \underset{\frown}{\boldsymbol{\Gamma}} = \underset{\frown}{\boldsymbol{\Phi}} + \underset{\approx}{\boldsymbol{i}} \cdot \underline{\boldsymbol{\nabla}} U_3 \tag{Eq. 3}$$

The clamped boundary conditions on $\partial\omega$ are :

$$\underset{\frown}{\boldsymbol{\Phi}} \cdot \underline{\boldsymbol{n}} = \underset{\sim}{\boldsymbol{0}} \quad \text{and} \quad U_3 = 0 \quad \text{on} \quad \partial\omega. \tag{Eq. 4}$$

The Bending-Gradient constitutive equations write as :

$$\underset{\sim}{\boldsymbol{\chi}} = \underset{\approx}{\boldsymbol{d}} : \underset{\sim}{\boldsymbol{M}}, \quad \underset{\frown}{\boldsymbol{\Gamma}} = \underset{\approx}{\boldsymbol{h}} \vdots \underset{\frown}{\boldsymbol{R}} \tag{Eq. 5}$$

where $\underset{\approx}{\boldsymbol{d}} = \underset{\approx}{\boldsymbol{D}}^{-1} = \left(\left\langle x_3^2 C^{\sigma}_{\alpha\beta\gamma\delta}(x_3)\right\rangle\right)^{-1}$ is the bending compliance tensor, the integration through the thickness of the plate is noted $\langle f(x_3)\rangle = \int_{-\frac{t}{2}}^{\frac{t}{2}} f(x_3)\, dx_3$, and $\underset{\approx}{\boldsymbol{h}}$ is the shear compliance tensor explicitly given in terms of the elastic components through the thickness of the plate, refer to [21]. It should be emphasized that $\underset{\approx}{\boldsymbol{h}}$ is symmetric and positive but it is definite only on the subspace $\underset{\frown}{\boldsymbol{\mathcal{S}}}$ orthogonal to its kernel.
The equilibrium equations of the Bending-Gradient theory write :

$$\begin{cases} \underset{\frown}{\boldsymbol{R}} - \underset{\approx}{\boldsymbol{P}}^{S} \vdots \left(\underset{\sim}{\boldsymbol{M}} \otimes \underline{\boldsymbol{\nabla}}\right) = \underset{\sim}{\boldsymbol{0}}, & \text{(Eq. 6a)} \\ \left(\underset{\approx}{\boldsymbol{i}} \vdots \underset{\frown}{\boldsymbol{R}}\right) \cdot \underline{\boldsymbol{\nabla}} + p_3 = 0. & \text{(Eq. 6b)} \end{cases}$$

where the sixth-order tensor $\underset{\approx}{\boldsymbol{P}}^{S}$ is the projection operator on $\underset{\frown}{\boldsymbol{\mathcal{S}}}$.

4.2. Variational formulation

Like 3D elasticity problems, the Bending-Gradient problem can be given a variational framework. For this purpose, the set KC^{BG} of kinematically compatible Bending-Gradient displacements are defined as :

$$KC^{\mathrm{BG}} = \left\{ \left(U_3, \underset{\frown}{\boldsymbol{\Phi}}\right)(x_1, x_2),\ \ \underset{\frown}{\boldsymbol{\Phi}} \in \underset{\frown}{\boldsymbol{\mathcal{S}}},\ \ (x_1, x_2) \in \omega, \quad \text{such that (Eq. 4)} \right\}, \tag{Eq. 7}$$

The theorem of the minimum of the potential energy says that the solution $\left(U_3^{\mathrm{BG}}, \underset{\frown}{\boldsymbol{\Phi}}^{\mathrm{BG}}\right)$ of the Bending-Gradient problem achieves the minimum of the potential energy functional P^{BG} defined on KC^{BG} as :

$$P^{\mathrm{BG}} = \int_{\omega} w^{\mathrm{BG}}\left(\underset{\sim}{\boldsymbol{\chi}}, \underset{\frown}{\boldsymbol{\Gamma}}\right) d\omega - \int_{\omega} p_3 U_3 d\omega, \tag{Eq. 8}$$

where $\underset{\sim}{\boldsymbol{\chi}}$ and $\underset{\frown}{\boldsymbol{\Gamma}}$ are the generalized strains associated to the generalized displacements $\left(U_3, \underset{\frown}{\boldsymbol{\Phi}}\right)$ through the compatibility equations (Eq. 3) and w^{BG} is the Bending-Gradient strain energy density function given by :

$$w^{\mathrm{BG}}\left(\underset{\sim}{\boldsymbol{\chi}}, \underset{\frown}{\boldsymbol{\Gamma}}\right) = \frac{1}{2} \underset{\sim}{\boldsymbol{\chi}} : \underset{\approx}{\boldsymbol{D}} : \underset{\sim}{\boldsymbol{\chi}} + \frac{1}{2}{}^{T}\underset{\frown}{\boldsymbol{\Gamma}} \vdots \underset{\approx}{\boldsymbol{H}} \vdots \underset{\frown}{\boldsymbol{\Gamma}}. \tag{Eq. 9}$$

where the generalized shear stiffness tensor $\underset{\approx}{\boldsymbol{H}}$ is the Moore-Penrose pseudo inverse of $\underset{\approx}{\boldsymbol{h}}$.

5. Finite element discretization of the Bending-Gradient model

This section deals with the displacement finite element formulation of the Bending-Gradient model presented in the previous section. An eight-node isoparametric quadrilateral element with 7 d.o.f. at each nodal point will be presented. *BGFEAP* (Bending-Gradient Finite Element Analysis Program) is a code developed in the Laboratoire Navier. The code is written using standard Fortran 77 and is a development of the program MEF presented in [22]. For more details, refer to [21].

5.1. Methods for calculating shear stiffness matrix

As noted before, the shear compliance tensor $\underset{\approx}{\underset{\approx}{\boldsymbol{h}}}$ is symmetric and positive. It is definite on the subspace $\underset{\approx}{\boldsymbol{S}}$ whose dimension is between two and six depending on the elastic properties of the laminated plate. Hence, there are two possible numerical strategies to handle this problem. The first one is to introduce the constraint $\boldsymbol{\Phi} \in \underset{\approx}{\boldsymbol{S}}$ when the dimension of $\underset{\approx}{\boldsymbol{S}}$ is strictly lower than six. It is named the reduction method, presented and detailed in [21]. The second one is to regularize the problem by adding a small strictly positive compliance to the diagonal components of the exact shear compliance tensor $\underset{\approx}{\underset{\approx}{\boldsymbol{h}}}$, which becomes the invertible compliance $\underset{\approx}{\underset{\approx}{\boldsymbol{h}}}^{\xi}$. The two methods were adopted and implemented in the computer code.
The regularized method, denoted by BG FE-RG, will be detailed here and used in the calculation.

$$\left[\underset{\approx}{\underset{\approx}{\boldsymbol{H}}}^{\xi}\right] = \left[\underset{\approx}{\underset{\approx}{\boldsymbol{h}}}^{\xi}\right]^{-1} = \left(\left[\underset{\approx}{\underset{\approx}{\boldsymbol{h}}}\right] + \frac{\sqrt{\sum h^2_{\alpha\beta\gamma\delta\zeta\eta}}}{10^{\xi}} \left[\underset{\approx}{\underset{\approx}{\boldsymbol{I}}}\right] \right)^{-1} \qquad \text{(Eq. 10)}$$

where $\alpha = \beta = \gamma = \delta = \zeta = \eta = 1,2$, $\left[\underset{\approx}{\underset{\approx}{\boldsymbol{I}}}\right]$ is the identity 6×6-matrix and ξ is a positive parameter.
A parametric study was conducted in which the exponent ξ was varied between 1 and 8. We recommend to set ξ=3 unless in the case of a concentrated loading force applied on a thick plate (slenderness between 3 and 10) for which ξ=5 is recommended.

5.2. Geometry and displacement interpolations

The representation of the geometry of the finite element mesh is based on a quadrilateral master element defined in the (ξ, η) space as shown in Fig. 2.

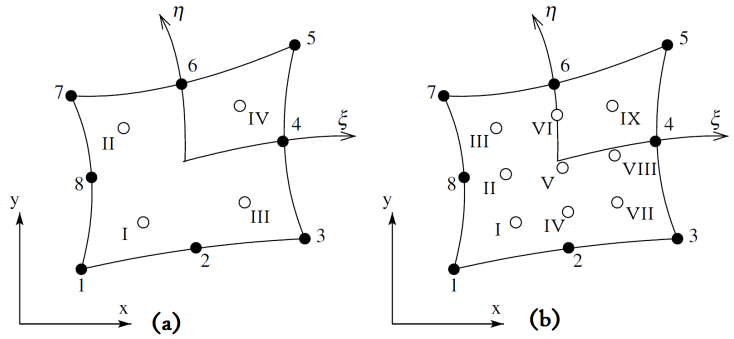

Fig. 2. The eight-node element a) with four second-order Gaussian stations b) with nine second-order Gaussian stations.

5.3. Weak formulation of the Bending-Gradient model

— The generalized displacement vector $[\delta]$ is defined as :

$$[\delta]^T = \left(U_3, \Phi_{111}, \Phi_{221}, \sqrt{2}\Phi_{121}, \Phi_{112}, \Phi_{222}, \sqrt{2}\Phi_{122}\right),$$

where $[X]^T$ is the transpose of $[X]$.

— The generalized strain vector $[E]$ defined as :

$$[E]^T = \left(\chi_{11}, \chi_{22}, \sqrt{2}\chi_{12}, \Gamma_{111}, \Gamma_{221}, \sqrt{2}\Gamma_{121}, \Gamma_{112}, \Gamma_{222}, \sqrt{2}\Gamma_{122}\right)^T$$

The strain field interpolation can be written as :

$$[E] = \sum_{i=1}^{8} [B_i]\,[\delta_i] = [B_1, \ldots, B_8]\,[\delta] \qquad \text{(Eq. 11)}$$

— Finally, the generalized stress vector $[\Sigma]$ is defined as :

$$[\Sigma]^T = \left(M_{11},\, M_{22},\, \sqrt{2}M_{12}, R_{111},\, R_{221},\, \sqrt{2}R_{121}, R_{112},\, R_{222},\, \sqrt{2}R_{122}\right)^T$$

With these notations, the Bending-Gradient constitutive equations (Eq. 5) can be rewritten as :

$$[E] = [S]\,[\Sigma]\,,\;\; [\Sigma] = [C]\,[E]\,, \qquad \text{(Eq. 12)}$$

where $[S]$ is the generalized compliance matrix and $[C] = [S]^{-1}$ is the generalized stiffness matrix.

5.4. Element stiffness matrix and nodal forces

The strain energy stored in the element will be expressed as follows :

$$W^e = \sum_{i=1}^{8}\sum_{j=1}^{8} \frac{1}{2}\int_{\omega^e} [\delta_i]^T\,[B_i]^T\,[C]\left[B_j\right]\left[\delta_j\right]\; dxdy = \sum_{i=1}^{8}\sum_{j=1}^{8} \frac{1}{2}\,[\delta_i]^T\left[K^e_{ij}\right]\left[\delta_j\right]$$

where the element stiffness matrix $\left[K^e_{ij}\right]$ is given by :

$$\left[K^e_{ij}\right] = \int_{\omega^e} [B_i]^T\,[C]\left[B_j\right]\; dxdy = \int_{\omega^e} \left(\left[B^\chi_i\right]^T[D]\left[B^\chi_j\right] + \left[B^\Gamma_i\right]^T\left[H^\xi\right]\left[B^\Gamma_j\right]\right)\; dxdy,$$

and that the work of the external forces in the element ω^e is : $\sum_{i=1}^{8} [\delta_i]^T\left[F^e_i\right]$

5.5. Bending-Gradient finite element with selective integration technique

It is well-known that the selective integration technique can be used to avoid shear locking in Reissner-Mindlin finite elements. In order to apply this technique to our model, the idea is to decompose the elasticity shear matrix $\underset{\approx}{\boldsymbol{H}}$ into two elasticity shear matrices $\left[\underset{\approx}{\boldsymbol{H}}^s\right]=\left[\underset{\approx}{\boldsymbol{H}}\right]\left[\underset{\approx}{\boldsymbol{P}}\right]$ and $\left[\underset{\approx}{\boldsymbol{H}}^d\right]=\left[\underset{\approx}{\boldsymbol{H}}\right]\left[\underset{\approx}{\boldsymbol{I}} - \underset{\approx}{\boldsymbol{P}}\right]$; $\left[\underset{\approx}{\boldsymbol{P}}\right]$ is the orthogonal projection operator on $\underset{\sim}{\boldsymbol{S}}^{(i)}$.
Let us introduce the following two-dimensional subspace $\underset{\sim}{\boldsymbol{S}}^{(i)} = \text{Span}\left\{\underset{\sim}{\boldsymbol{i}}^{(1)}, \underset{\sim}{\boldsymbol{i}}^{(2)}\right\}$ where $\underset{\sim}{\boldsymbol{i}}^{(1)} = \left(i^{(1)}_{\alpha\beta\gamma}\right) = \left(i_{1\gamma\beta\alpha}\right)$ and $\underset{\sim}{\boldsymbol{i}}^{(2)} = \left(i^{(2)}_{\alpha\beta\gamma}\right) = \left(i_{2\gamma\beta\alpha}\right)$ The part of the shear energy $\frac{1}{2}{}^T\underset{\sim}{\boldsymbol{\Gamma}} \vdots \underset{\approx}{\boldsymbol{H}} \vdots \underset{\sim}{\boldsymbol{\Gamma}}$ associated to matrix $\left[\underset{\approx}{\boldsymbol{H}}^s\right]$ is numerically integrated with four Gauss points while the part associated to matrix $\left[\underset{\approx}{\boldsymbol{H}}^d\right]$ is subjected to full integration with nine Gauss points (or more, the results are the same).
The space generated by all possible $\underset{\sim}{\boldsymbol{\Phi}}$ is orthogonally decomposed, in the sense of the scalar product defined by $\underset{\approx}{\boldsymbol{H}}$, into the subspace $\underset{\sim}{\boldsymbol{S}}^{(i)}$ which is generated by the $\underset{\sim}{\boldsymbol{\Phi}}$ of the form $\underset{\approx}{\boldsymbol{i}}\cdot\underline{\boldsymbol{\nabla}}U_3$, and its orthogonal counterpart. This method is detailed in [21].

6. Examples and numerical results

In this part, all comparisons are made between Bending-Gradient finite element when using the regularized method, denoted by BG FE-RG, Bending-Gradient analytical solution, *LS1* finite element and plate bending FE model in order to assess the performances of the new model. Moreover, the Bending-Gradient finite element model converges to the exact constant value for bending, twisting and shear patch tests, specially for small slenderness ratio (L/h). In addition, same results were obtained between the Bending-Gradient FE-RG and the exact analytical solution when considering a multilayered plate subjected to a cylindrical bending. The 2D FE calculations are performed with the commercial *ABAQUS* software. The following notations are used :
$\overline{U_3} = \dfrac{U_3}{L}, \quad \overline{R}_{\alpha\beta\gamma} = \dfrac{R_{\alpha\beta\gamma}}{EL^2}, \quad \overline{Q}_\alpha = \dfrac{Q_\alpha}{EL^2}, \quad \overline{M}_{\alpha\beta} = \dfrac{M_{\alpha\beta}}{EL}$

6.1. Comparison between Bending-Gradient FE, *LS1* and Abaqus 2D FE

In this section, 2 different cases are presented, the first case is a simply supported square plate with a uniformly distributed load and the second case is a cylindrical bending of a simply supported plate. The commercial ABAQUS software has been used with S8R element (2D 8-node quadratic shell element with reduced integration). Comparisons are made between Bending-Gradient FE using the regularized method, *LS1* and Abaqus 2D FE composite layup module with the same mesh refinement.

6.1.1. First case

The laminate under consideration is a square plate with a length and width of L=10 in the X and Y directions. The thickness of the laminate, following z direction, is equal to h=4e and the middle plane of the plate is located at z=0. The plate is simply supported on its 4 edges, and is subjected to a uniform load equal to $0.48E$. The slenderness ratio L/h is set equal to 4.

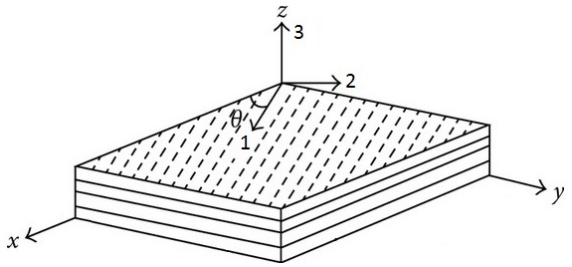

Fig. 3. Description of fiber orientation axes and angle.

The material properties are as in [23] and [24]. For the first and fourth layers, the fiber orientation is 30° and the elastic constants are :
E_1=140 000E, E_2=E_3=15 000E, G_{12}=G_{13}=G_{23}=5 850E, ν_{12}=ν_{13}=ν_{23}=0.21.
where 1, 2 and 3 refer, respectively, to the fiber, transverse, and thickness direction as shown in Fig. 3
For the second and third layers, the fiber orientation is −30° and the elastic constants are :
E_1=160 000E, E_2=E_3=8 500E, G_{12}=G_{13}=4 100E, G_{23}=2 800E, ν_{12}=ν_{13}=0.33 , ν_{23}=0.5.

In Fig. 4, we plot the distribution of moments $\overline{M}_{11}$ and $\overline{M}_{22}$ and shear forces $\overline{Q}_1$ and $\overline{Q}_2$, at Y=$L/2$ as predicted by Bending-Gradient FE, *LS1* and Abaqus 2D FE. In Fig. 5, we plot the deflection $\overline{U}_3$ at Y=$L/2$ as predicted by Bending-Gradient FE, *LS1* and Abaqus 2D FE. In Fig. 6, we plot the distribution of moment of torsion $\overline{M}_{12}$, at A) diagonal between X=0, Y=0 and X=L, Y=L and B) diagonal between X=0, Y=L and X=L, Y=0, as predicted by BG FE-RG, *LS1* and Abaqus 2D FE.

6.1.2. Second case

The laminate used in this example is composed of 8 layers. Each layer is made of unidirectional fiber-reinforced material oriented at θ relative to the direction X. All plies are perfectly bounded. The constitutive behavior of a ply is assumed to be transversely isotropic along the direction of the fibers and engineering constants are chosen similar to those of [25]. The plate slenderness ratio (L/h) is set equal to 4. The thickness of each layer is set equal to 0.625, the fiber orientation is [0°, −45°, 90°, 45°]s and the elastic constants are :
E_1=25E, E_2=E_3=1E, G_{12}=G_{13}=0.5E, G_{23}=$\dfrac{E_2}{2(1+\nu_{32})}$=0.4$E$, ν_{12}=ν_{13}=ν_{23}=0.25.
where 1, 2 and 3 refer, respectively, to the fiber, transverse, and thickness direction as shown in Fig. 3
The laminate is subjected to a cylindrical bending of a simply supported composite laminates (Fig. 7), with L=20 and where the plate is invariant and infinite in Y direction and a uniformly distributed load equal to $0.05E$ is applied. The particular choice of 3D boundary conditions shown in Fig. 7 and

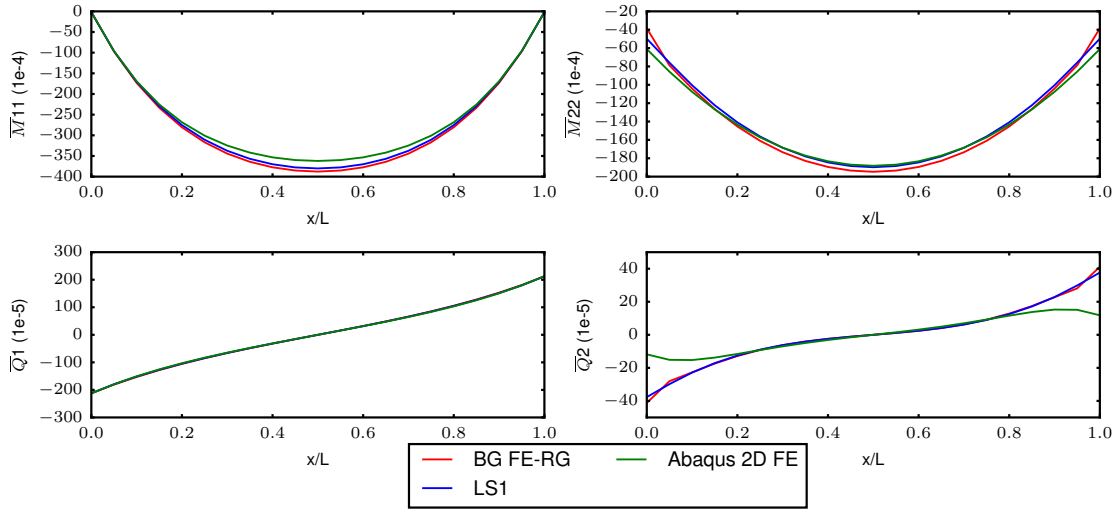

Fig. 4. Distribution of moments $\overline{M}_{11}$ and $\overline{M}_{22}$ and shear forces $\overline{Q}_1$ and $\overline{Q}_2$ at Y=L/2, predicted by BG FE-RG, LS1 *and Abaqus 2D FE for* 30°/ − 30°/ − 30°/30°.

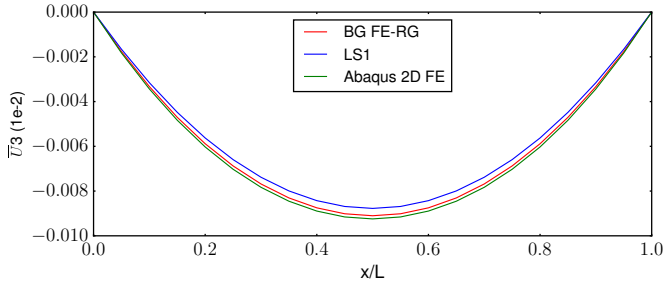

Fig. 5. Deflection $\overline{U}_3$ at Y=L/2, predicted by BG FE-RG, LS1 *and Abaqus 2D FE for* 30°/ − 30°/ − 30°/30°.

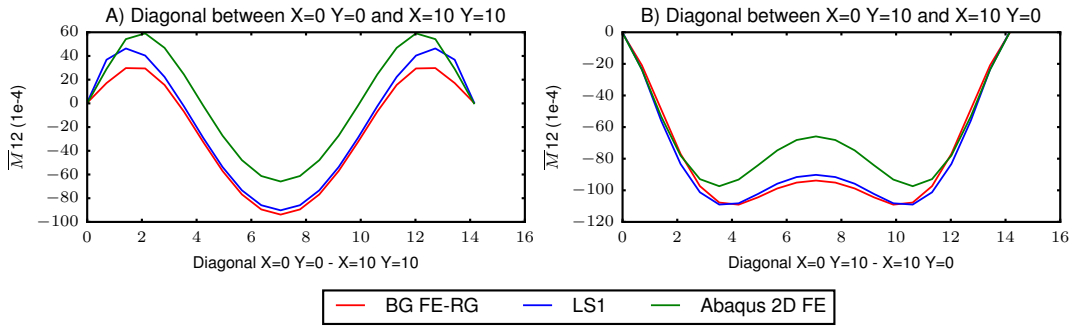

Fig. 6. Distribution of moment of torsion $\overline{M}_{12}$ at A) diagonal between X=0, Y=0 and X=L, Y=L and B) diagonal between X=0, Y=L and X=L, Y=0, predicted by BG FE-RG, LS1 *and Abaqus 2D FE for* 30°/ − 30°/ − 30°/30°.

the invariance of the solution in Y direction enable a variable separation between z and X, and the derivation of a closed form solution.

In this example, the plate is studied with respect to the bending direction which is the plate's overall configuration rotated relative to z axis. In table 1, the relative difference for deflection and moments M_{22} and M_{12} are presented at $X = L/2$ for *LS1* (reference solution), BG FE-RG and Abaqus 2D FE. It should be noted that the relative difference between *LS1* and BG FE-RG is calculated as follows :

$$\Delta^{BG\ \ FE-RG/LS1} = \frac{BG\ \ (FE-RG) - LS1}{LS1}$$

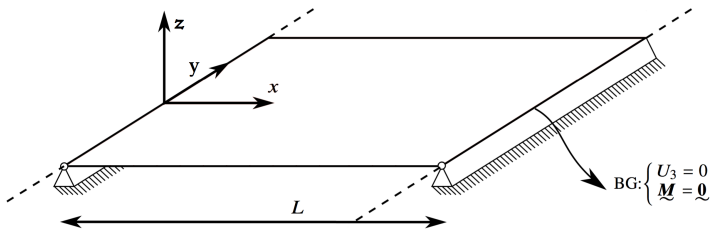

Fig. 7. Description of laminated plate configuration for cylindrical bending.

$[0°,-45°,90°,45°]$s	Model	U_3	M_{22}	M_{12}
+0°	$\Delta^{BG\ \ FE-RG/LS1}$	0.003475936	-0.00754134	-0.013216837
	$\Delta^{Abaqus\ 2D\ FE/LS1}$	0.00155615	0.087379228	0.036639273
+15°	$\Delta^{BG\ \ FE-RG/LS1}$	0.004379947	-0.003530737	0.014864941
	$\Delta^{Abaqus\ 2D\ FE/LS1}$	0.009343008	0.113267216	-0.447439409
+30°	$\Delta^{BG\ \ FE-RG/LS1}$	0.005373494	0.000160823	0.008319649
	$\Delta^{Abaqus\ 2D\ FE/LS1}$	0.045862651	-0.013292055	-0.392058748
+45°	$\Delta^{BG\ \ FE-RG/LS1}$	0.006357895	0.002014597	0.00720255
	$\Delta^{Abaqus\ 2D\ FE/LS1}$	0.058105263	-0.125204338	-0.363731131

Tab. 1. Relative difference between LS1 *(reference solution) and BG FE-RG and Abaqus 2D FE for plate's overall configuration and bending direction.*

It should be noted that the values obtained for M_{11}, Q_1 and Q_2 are the same for the 3 different models. According to the results obtained, we can conclude that the Bending-Gradient finite element converge to the reference *LS1* solution with a good accuracy for deflection, moments and shear forces for all plate's configuration and bending direction, unlike Abaqus 2D FE which cannot predict plate's behavior for all cases.
It is seen that for these two cases, the Bending-Gradient FE model can efficiently predict the same response solution as the *LS1* (which was validated in [10, 11, 12, 13, 14, 26, 15, 16, 17, 18, 19, 20]) and Abaqus 2D FE. It should be noted, for thick plate (L/h=4), that Abaqus 2D FE is not very efficient as shown by the results above. Accordingly, the new Bending-Gradient finite element has been proved as an efficient and reliable model for the study of complex multilayered structures with minimum computational time.

7. Conclusion

In this paper, the Bending-Gradient model for laminated plates, dedicated for out-of-plane load, and its finite element, are presented. An eight-node isoparametric quadrilateral finite element with 7 degrees of freedom at each nodal point has been formulated. The current finite element program called BGFEAP has been developed in order to take into account the Bending-Gradient theory. The new proposed finite element program presents a 2D type data structure that provides several advantages over a conventional 3D finite element model : simplified input data, ease of results' interpretation and a huge reduction of calculation time. In the light of the foregoing, this new model has passed patch test, as well as same results were obtained when comparing Bending-Gradient FE to analytical solution of the Bending-Gradient model. In addition, the performance of this new element has been compared with those of a standard 2D FE and *LS1* layerwise model. It has been demonstrated that the proposed Bending-Gradient FE model has better performance because it is able to reproduce almost

the same resutls as conventional FE and layerwise model, at a reduced cost.

Références

[1] E. Reissner « On the Theory of Bending of Elastic Plates », *Journal of Mathematics and Physics* Vol. 23 n° 1-4, pp. 184–191, 1944, ISSN 1467-9590.

[2] A. Lebée, K. Sab « On the Generalization of Reissner Plate Theory to Laminated Plates, Part I : Theory », *Journal of Elasticity* Vol. 126 n° 1, pp. 39–66, 2017, ISSN 1573-2681.

[3] A. Lebée, K. Sab « On the Generalization of Reissner Plate Theory to Laminated Plates, Part II : Comparison with the Bending-Gradient Theory », *Journal of Elasticity* Vol. 126 n° 1, pp. 67–94, 2017, ISSN 1573-2681.

[4] A. Lebée, K. Sab « A Bending-Gradient model for thick plates. Part I : Theory », *International Journal of Solids and Structures* Vol. 48, pp. 2878–2888, 2011.

[5] A. Lebée, K. Sab « A Bending-Gradient model for thick plates. Part II : Closed-form solutions for cylindrical bending of laminates », *International Journal of Solids and Structures* Vol. 48, pp. 2889–2901, 2011.

[6] A. Lebée, K. Sab « Homogenization of thick periodic plates : Application of the Bending-Gradient plate theory to a folded core sandwich panel », *International Journal of Solids and Structures* Vol. 49, pp. 2778–2792, 2012.

[7] K. Sab, A. Lebée, Homogenization of Heterogeneous Thin and Thick Plates, Wiley-ISTE, 2015.

[8] A. Lebée, K. Sab, The Bending-Gradient Theory for Laminates and In-Plane Periodic Plates, chap. The Bending-Gradient theory for laminates and in-plane periodic plates, Springer International Publishing, Cham, ISBN 978-3-319-42277-0, , pp. 113–148, 2017.

[9] O. Perret, A. Lebée, C. Douthe, K. Sab « The Bending-Gradient theory for the linear buckling of thick plates : Application to Cross Laminated Timber panels », *International Journal of Solids and Structures* Vol. 87, pp. 139–152, 2016, ISSN 0020-7683.

[10] T. Naciri, A. Ehrlacher, A. Chabot « Interlaminar stress analysis with a new Multiparticle modelization of Multi-layered Materials (M4) », *Composites Science and Technology* Vol. 58, pp. 337–343, 1998.

[11] R. P. Carreira, J. F. Caron, A. Diaz Diaz « Model of multilayered materials for interface stresses estimation and validation by finite element calculations », *Mechanics of Materials* Vol. 34, pp. 217–230, 2002.

[12] A. Diaz Diaz, J. F. Caron, R. P. Carreira « Software application for evaluating interfacial stresses in inelastic symmetrical laminates with free edges », *Composite Structures* Vol. 58, pp. 195–208, 2002.

[13] J. F. Caron, A. Diaz Diaz, R. P. Carreira, A. Chabot, A. Ehrlacher « Multi-particle modelling for the prediction of delamination in multi-layered materials », *Composites Science and Technology* Vol. 66, pp. 755–765, 2006.

[14] V. T. Nguyen, J. F. Caron « A new finite element for free edge effect analysis in laminated composites », *Computers and Structures* Vol. 84, pp. 1538–1546, 2006.

[15] N. Saeedi, K. Sab, J. F. Caron « Delaminated multilayered plates under uniaxial extension. Part I : Analytical analysis using a layerwise stress approach », *International Journal of Solids and Structures* Vol. 49, pp. 3711–3726, 2012.

[16] N. Saeedi, K. Sab, J. F. Caron « Delaminated multilayered plates under uniaxial extension. Part II : Very efficient layerwise mesh strategy for the prediction of delamination onset », *International Journal of Solids and Structures* Vol. 49, pp. 3727–3740, 2012.

[17] N. Saeedi, K. Sab, J. F. Caron « Cylindrical bending of multilayered plates with multi-delamination via a layerwise stress approach », *Composite Structures* Vol. 95, pp. 728–739, 2013.

[18] N. Saeedi, K. Sab, J. F. Caron « Stress analysis of long multilayered plates subjected to invariant loading : Analytical solutions by a layerwise stress model », *Composite Structures* Vol. 100, pp. 307–322, 2013.

[19] A. Lerpiniere, J. Caron, A. Diaz Diaz, K. Sab « The *LS*1 model for delamination propagation in multilayered materials at $0°/\theta°$ interfaces : A comparison between experimental and finite elements strain energy release rates », *International Journal of Solids and Structures* Vol. 51, pp. 3973–3986, 2014.

[20] R. Baroud, K. Sab, J.-F. Caron, F. Kaddah « A statically compatible layerwise stress model for the analysis of multilayered plates », *International Journal of Solids and Structures* Vol. 96, pp. 11–24, 2016, ISSN 0020-7683.

[21] R. Baroud, K. Sab, A. Lebée, F. Kaddah « Finite-Element Modeling of laminated plates using the Bending-Gradient theory », *submitted paper* Vol. , pp. , 2017.

[22] G. . Dhatt, G. Touzot, Une présentation de la méthode des éléments finis, Maloine, Paris, 1984.

[23] A. Wang, F. W. Crossman « Some New Results on Edge Effect in Symmetric Composite Laminates », 1977.

[24] N. Pagano, R. Pipes « Composite Laminates Under Uniform Axial Extension », *Journal of Composite Materials* Vol. , pp. 538–548, 1970.

[25] N. Pagano « Exact Solutions for Composite Laminates in Cylindrical Bending », *Journal of Composite Materials* Vol. 3 n° 3, pp. 398–411, 1969.

[26] J. Dallot, K. Sab « Limit analysis of multi-layered plates. Part II : Shear effects », *Journal of the Mechanics and Physics of Solids* Vol. 56, pp. 561–580, 2008.